Bat Algorithm for Attractor Reconstruction of Low-Dimensional Chaotic Maps from Time Series

Akemi Gálvez
Dept. of Applied Math. & Comp. Sci.
University of Cantabria
Santander, Spain
galveza@unican.es

Sara Pérez-Carabaza
Dept. of Applied Math. & Comp. Sci.
University of Cantabria
Santander, Spain
sara.perezcarabaza@unican.es

Andrés Iglesias*
Dept. of Applied Math. & Comp. Sci.
University of Cantabria
Santander, Spain
iglesias@unican.es
(*Corresponding author)

***Abstract*—Reconstructing the attractors of unknown chaotic systems from time series data presents a formidable challenge with broad applications across various disciplines. In this paper, we propose a swarm intelligence approach to address this challenge, focusing specifically on low-dimensional chaotic maps. Our approach is based on the bat algorithm, a renowned bio-inspired optimization technique well-suited for continuous optimization tasks. We evaluate the effectiveness and validity of our proposed approach by applying it to two distinct examples of chaotic maps: the Burger map and the Duffing map. Through comprehensive experimentation, we showcase the satisfactory performance of our method in reconstructing attractors from time series data. Based on our empirical findings, we conclude that our approach holds significant promise for the reconstruction of attractors of low-dimensional chaotic maps using time series data.**

***Index Terms*—Dynamical systems, chaotic maps, attractor reconstruction, time series, swarm intelligence, bat algorithm.**

I. Introduction

Nowadays, dynamical systems are extensively employed for accurately describing the evolution of various natural and artificial systems, utilizing both discrete and continuous mathematical equations [3], [36]. The system evolution analysis typically involves studying the trajectories of system variables, referred to as orbits [2], [7]. While orbit analysis is crucial for understanding dynamical systems, it poses a significant challenge, particularly in the case of chaotic systems [19], [40]. As a result, numerous techniques have been developed to enhance our comprehension of dynamical system behavior [9], [17], [30]. Among these techniques, delay-coordinate embedding has shown relative success for some instances of dynamical systems [1], [8], [27]. However, embedding methods suffer from drawbacks such as sensitivity to parameter selection, susceptibility to noise in measured data, and limitations regarding system dimensionality [6].

To address these challenges, researchers have explored various extensions and alternative techniques. Recent advancements include the utilization of autoencoders for learning embeddings [25], [34], as well as the consideration of variational Bayes filters [26]. Additionally, artificial intelligence (AI) approaches have garnered attention, encompassing techniques such as kernel methods, support vector machines, and neural networks [20], [31], [35]. Furthermore, machine learning approaches [13], [28] and deep learning [29] have emerged as promising avenues for analyzing dynamical systems.

This paper addresses the problem of reconstructing periodic and chaotic attractors of dynamical systems using time series data. Given the broad scope of this problem, it cannot be fully addressed within a single paper. Therefore, we narrow our focus to discrete systems, specifically low-dimensional chaotic maps. Our approach formulates the problem as a continuous nonlinear optimization task, which we tackle using the bat algorithm, a popular bio-inspired swarm intelligence method praised for its effectiveness in continuous optimization tasks. To evaluate the performance of our method, we conduct computational experiments, applying it to two representative examples of chaotic maps: the Burger map and the Duffing map. The experimental outcomes show the ability of our approach to accurately reconstruct various system behaviors.

The paper is structured as follows: Section II presents the optimization problem formulation and introduces the bat algorithm as the chosen bio-inspired optimization method. Section III provides detailed descriptions of the two illustrative examples of chaotic maps. The experimental results are discussed in Section IV. The paper concludes with a summary of findings and suggestions for future research directions.

II. The Proposed Method

A. Problem To be Solved

The problem posed in this paper can be stated as follows: given sets of data points, $\{x_n, y_n\}_{n=1,\ldots,N}$, derived from time series data of an unknown chaotic map with diverse attractors, our objective is to reconstruct the attractors effectively. Specifically, we focus on the scenario involving low-dimensional chaotic maps. In this paper, we assume that any map $\mathcal{M}$ can be represented as a linear combination of functions from a given family $\{\phi_1(x,y), \phi_2(x,y), \ldots, \phi_m(x,y)\}$, i.e.:

$$\mathcal{M}(x,y) = \sum_{k=1}^{m} \lambda_k \phi_k(x,y) \tag{1}$$

Research work funded by Project PDE-GIR (No. 778035) of the European Union Horizon 2020 research and innovation programme under the Marie Sklodowska-Curie Actions, and project PID2021-127073OB-I00 of the MCIN/AEI/10.13039/501100011033/FEDER,EU, Spanish Ministry of Science and Innovation.

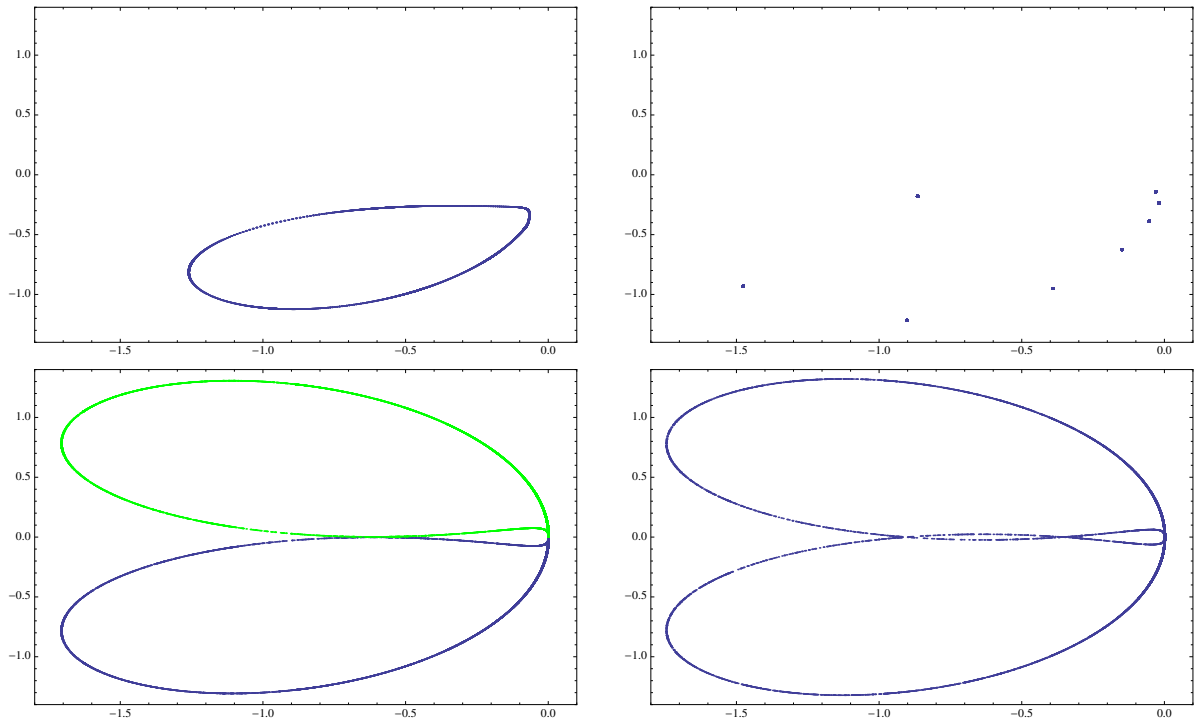

Fig. 1. Different behaviors of the Burger map (for $\nu = 1$) as a function of μ (top-bottom, left-right): (t-l) quasiperiodicity, $\mu = 0.62$; (t-r) period-8 orbit, $\mu = 0.67$; (b-l) two chaotic attractors, $\mu = 0.71$ (only one color is obtained for each initial condition); (b-r) chaotic attractor, $\mu = 0.72$.

Then, the problem consists of computing the parameters of the linear combination that minimize the error between the original data, (x_n, y_n), and the reconstructed data, $(\bar{x}_n, \bar{y}_n)$, leading to the functional:

$$min \left[\sum_{i=1}^{N} \left(\sum_{k=1}^{m} \lambda_k \phi_k(x_i, y_i) - (\bar{x}_i, \bar{y}_i) \right) \right] \tag{2}$$

which is a nonlinear optimization problem for nonlinear functions $\phi_k(x, y)$. In this paper, the minimization problem in Eq. (2) is solved through the bat algorithm, described below.

B. The Bat Algorithm

The *bat algorithm* is a well-known swarm intelligence technique employed for tackling continuous optimization problems, drawing inspiration from certain aspects of the social behavior observed in microbats [43], [45]. Microbats utilize a specialized form of sonar known as echolocation for various tasks, including motion planning, prey detection, and obstacle avoidance. The algorithm initializes with a population of individuals, or bats, randomly dispersed throughout the search space. These bats engage in extensive exploration to locate the best solution, a metric associated with solution quality. During movement, the dynamics of each bat i at iteration g is governed by its frequency f_i^g, location $\mathbf{x}_i^g$, and velocity $\mathbf{v}_i^g$, determined by the following equations:

$$f_i^g = f_{min}^g + \beta(f_{max}^g - f_{min}^g) \tag{3}$$

$$\mathbf{v}_i^g = \mathbf{v}_i^{g-1} + [\mathbf{x}_i^{g-1} - \mathbf{x}^*] f_i^g \tag{4}$$

$$\mathbf{x}_i^g = \mathbf{x}_i^{g-1} + \mathbf{v}_i^g \tag{5}$$

Here, β represents a uniformly distributed random variable in the interval $[0, 1]$, and $\mathbf{x}^*$ denotes the current global best location, obtained by evaluating the fitness function for all bats and subsequently ranking the corresponding fitness values. The algorithm further performs a local search in the vicinity of the current best solution through a random walk described as $\mathbf{x}_{new} = \mathbf{x}_{old} + \epsilon \mathcal{A}^g$, where ϵ is a uniformly distributed random number in $[-1, 1]$, and $\mathcal{A}^g =< \mathcal{A}_i^g >$ represents the average loudness of all bats in the population at generation g. Any new solution that improves upon the previous best solution is accepted with a probability dependent on the loudness value. Upon acceptance, the pulse rate is augmented according to the law $r_i^{g+1} = r_i^0[1 - \exp(-\gamma g)]$, where γ is a method parameter. Concurrently, the loudness diminishes following the evolution rule $\mathcal{A}_i^{g+1} = \alpha \mathcal{A}_i^g$, with α representing another parameter of the method. This iterative process continues for a maximum number of iterations, denoted as $\mathcal{G}_{max}$, that is also a parameter of the method.

The algorithm facilitates individual bats to possess varying loudness and pulse emission rate values, initialized randomly with $\mathcal{A}_i^0 \in (0, 2)$ for loudness and $r_i^0 \in [0, 1]$ for the emission rate. Both parameters are updated only when new solutions improve the current ones. The bat algorithm is chosen in this work over alternative methods due to its demonstrated effectiveness in numerous difficult optimization problems, as evidenced in some previous papers by the authors (e.g., see [5], [10]–[12], [22], [23], [37]–[39]). For an in-depth review of the bat algorithm and its diverse applications, interested readers are also referred to [44].

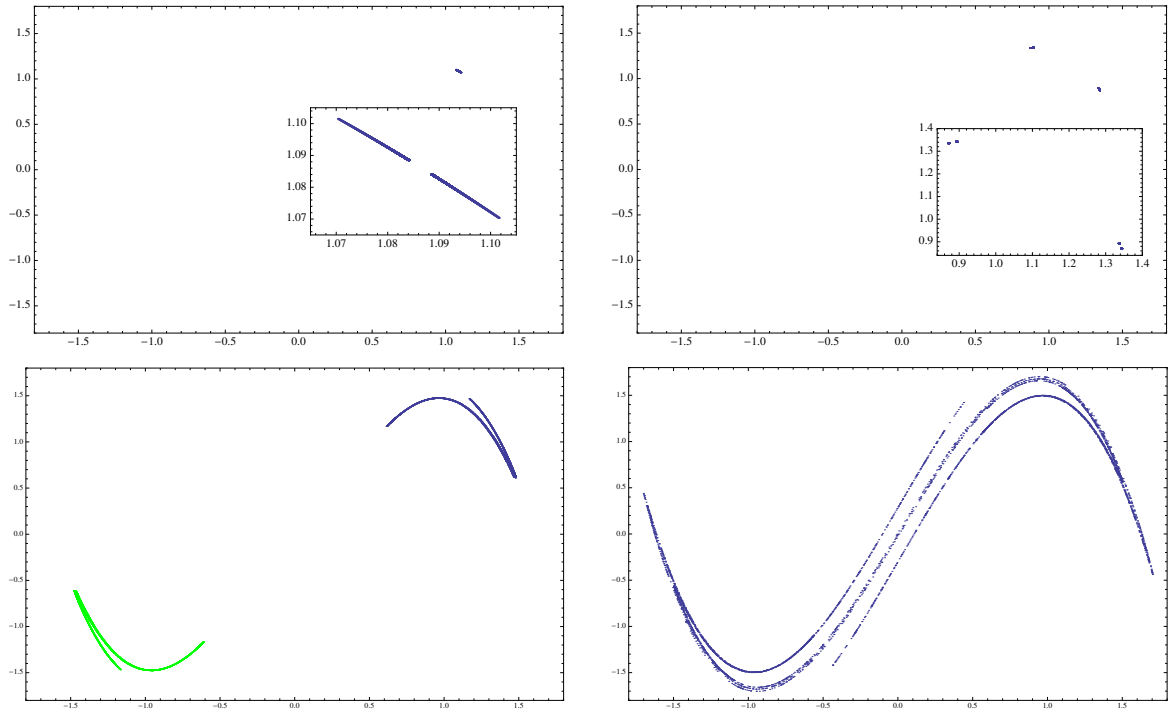

Fig. 2. Different behaviors of the Duffing map (for $b = 0.18$) as a function of a (top-bottom, left-right): (t-l) two segment attractors, $a = 2.36$; (t-r) four segment attractors, $a = 2.57$; (b-l) two chaotic attractors, $a = 2.71$ (only one color is obtained for each initial condition); (b-r) chaotic attractor, $a = 2.75$.

III. Illustrative Examples

To analyze the performance of the proposed method, it has been applied to several discrete chaotic systems. However, due to space constraints, this paper focuses on two illustrative examples of chaotic maps: the Burger map and the Duffing map. They are briefly described in next paragraphs.

A. The Burger Map

The Burger map is a dynamical system derived by discretization in [41], [42] of two coupled ordinary differential equations used to analyze hydrodynamic flows in [4]. It is defined by the following evolution equations:

$$\left.\begin{array}{rl} x_{n+1} = & (1-\nu)x_n - y_n^2 \\ y_{n+1} = & (1+\mu)y_n + x_n y_n \end{array}\right\} \quad (6)$$

Considering the case $\nu = 1$, the map becomes:

$$\left.\begin{array}{rl} x_{n+1} = & -y_n^2 \\ y_{n+1} = & (1+\mu)y_n + x_n y_n \end{array}\right\} \quad (7)$$

Varying the value of parameter μ, the Burger map in Eq. (7) exhibits different behaviors [14]. Some of them are shown in Fig. 1. Quasiperiodicity is observed for $\mu = 0.62$, shown in Fig. 1(top-left), while a period-8 orbit is obtained for $\mu = 0.67$, see Fig. 1(top-right). Increasing the value of μ leads to chaotic behavior, for instance, for $\mu = 0.71$, when the system exhibits a pair of strange attractors, represented in blue and green in Fig. 1(bottom-left), that are symmetric with respect to the axis $y = 0$. Depending on the initial condition, we obtain one of these attractors. Increasing the value of μ even further, the two attractors merge into a single attractor, shown in Fig. 1(bottom-right) for $\mu = 0.72$.

B. The Duffing Map

The Duffing map is the discrete version of the Duffing oscillator [21], and is given by:

$$\left.\begin{array}{rl} x_{n+1} = & y_n \\ y_{n+1} = & -bx_n + ay_n - y_n^3 \end{array}\right\} \quad (8)$$

which depends on two parameters a and b. Taking $b = 0.18$, different behaviors for the Duffing map can be obtained as a function of parameter a [15]. A period-doubling sequence to chaos can be found, with two segments for $a = 2.36$, depicted in Fig. 2(top-left) and enlarged in the inset graphic for better visualization; four segments for $a = 2.57$, see Fig. 2(top-right); and so on, leading to a pair of strange attractors for $a = 2.71$, represented in blue and green in Fig. 2(bottom-left). The attractors can be independently attained depending on the initial condition. Increasing the value to $a = 2.75$, the system exhibits an attractor-merging crisis where the two strange attractors become connected and merged into a single one, shown in Fig. 2(bottom-right).

IV. Results and Discussion

A. Computational Experiments and Parameter Tuning

We applied the method described in Sect. II-B to the optimization problem given by Eq. (2) for the two examples described in Sect. III. The initial population is comprised by 100 potential solutions expressed as a linear combination of the family of functions: $\phi_{p,q}(x,y) = x^p y^q$, $p, q = 0, \ldots, 3$.

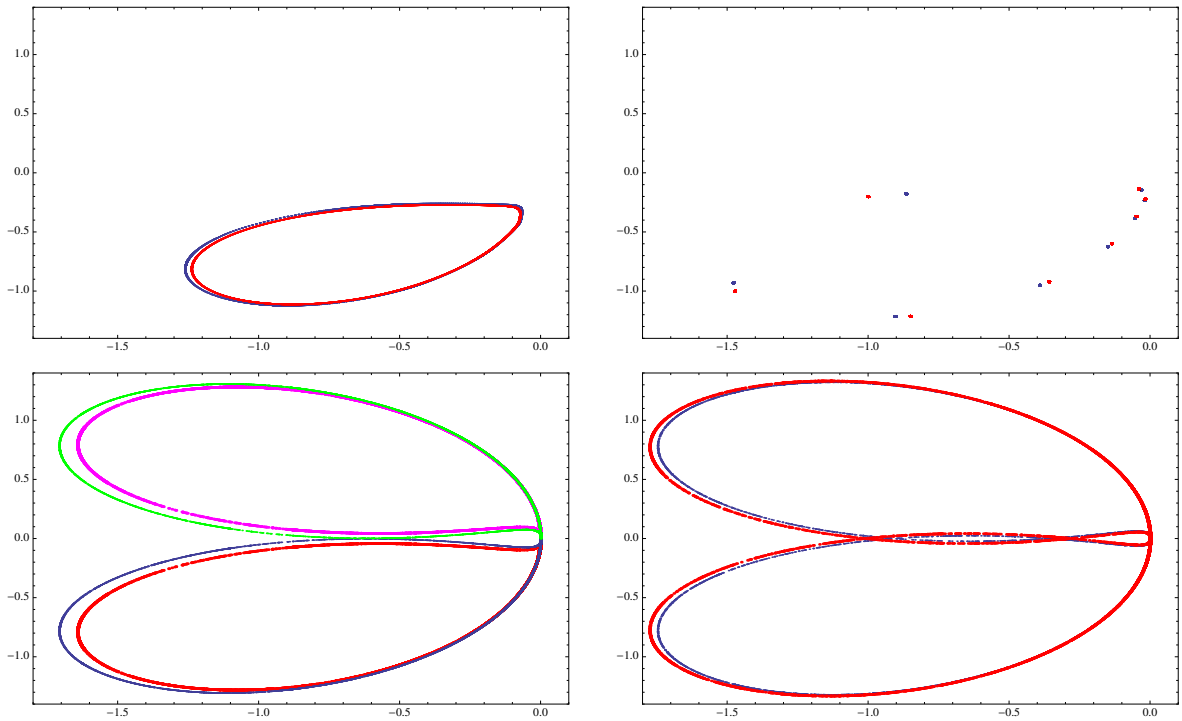

Fig. 3. Attractor reconstruction of the Burger map from the original time series data in Fig. 1, displayed in blue. The reconstructed data are displayed in red for easier visual comparison: (t-l) quasiperiodicity; (t-r): period-8 orbit; (b-l) two independent chaotic attractors (the second one is displayed in green (original data) and magenta (reconstructed data)); (b-r) a single chaotic attractor.

Accordingly, any potential solution can be written as: $\mathbf{C}_1 + \mathbf{C}_2 x + \mathbf{C}_3 y + \mathbf{C}_4 x^2 + \mathbf{C}_5 xy + \mathbf{C}_6 y^2 + \mathbf{C}_7 x^3 + \mathbf{C}_8 x^2 y + \mathbf{C}_9 xy^2 + \mathbf{C}_{10} y^3$. Here, $\mathbf{C}_i$ are two-dimensional vectors, resulting in 20 parameters to be optimized. Using the time series data from Figs. 1 and 2, we apply the bat algorithm to minimize the 10 parameter vectors $\mathbf{C}_i$ as per Eq. (2).

Regarding the parameter tuning, the bat algorithm is executed for a fixed number of iterations, denoted as $\mathcal{G}_{max}$. Through multiple simulations, we determined that $\mathcal{G}_{max} = 1,000$ provides sufficient convergence across all cases. The remaining parameters of the bat algorithm are empirically chosen and set as follows: $\mathcal{A}^0 = 0.5$, $r^0 = 0.25$, $\alpha = 0.5$, and $\gamma = 0.3$. Subsequently, the bat algorithm is executed, and the best individual at the final iteration is designated as the solution to the optimization problem.

An important observation arises from the fact that some parameter values $\mathbf{C}_i$ are exceedingly small, rendering their contribution to the solution negligible and introducing noise into the system. To address this, we discard all coefficients smaller than a prescribed threshold, set at 10^{-3} in this work. This filtering strategy is applied not only at the final iteration for the ultimate solution but across all iterations to alleviate computational burden while maintaining result accuracy.

Finally, to evaluate the performance of the method, we employ the root-mean-square error (RMSE) metric from Eq. (2), defined as $RMSE = \sqrt{\sum_{i=1}^{N} \frac{(D_i - \bar{D}_i)^2}{N}}$, where D_i and $\bar{D}_i$ denote the observed and the predicted values, respectively, and N indicates the sample size.

B. Results

The graphical results of our attractor reconstruction technique applied to the diverse behaviors exhibited by the Burger map and the Duffing map, as depicted in Figs. 1 and 2, are presented in Figs. 3 and 4, respectively. In each instance, the reconstructed attractor (in red) is juxtaposed with the original attractor (in blue) for convenient visual comparison. Our method has successfully reconstructed all observed behaviors with good accuracy. This encompasses not only regular (periodic) behaviors, such as the period-8 orbit of the Burger map in Fig. 3(top-right), but also other dynamical behaviors such as periodicity for the Burger map in Fig. 3(top-left), or the two-segment and four-segment attractors of the Duffing map shown in Figs. 4(top-left) and (top-right), respectively.

The chaotic attractors have also been retrieved with notable fidelity. For instance, our method accurately reconstructed the general shape and behavior of the two strange attractors of the Burger map, as depicted in Fig. 3(bottom-left), as well as the single chaotic attractor showcased in Fig. 3(bottom-right). Similar results are obtained for the Duffing map, as evidenced in Figs. 4(bottom-left) and (bottom-right), respectively.

These promising graphical outcomes are corroborated by numerical results. The RMSE errors range from 10^{-1} to 10^{-3} across all cases, contingent upon various factors. These values confirm the efficacy and robustness of our proposed technique. In light of these findings, we conclude that our approach is well-suited for reconstructing attractors of low-dimensional chaotic maps from time series data.

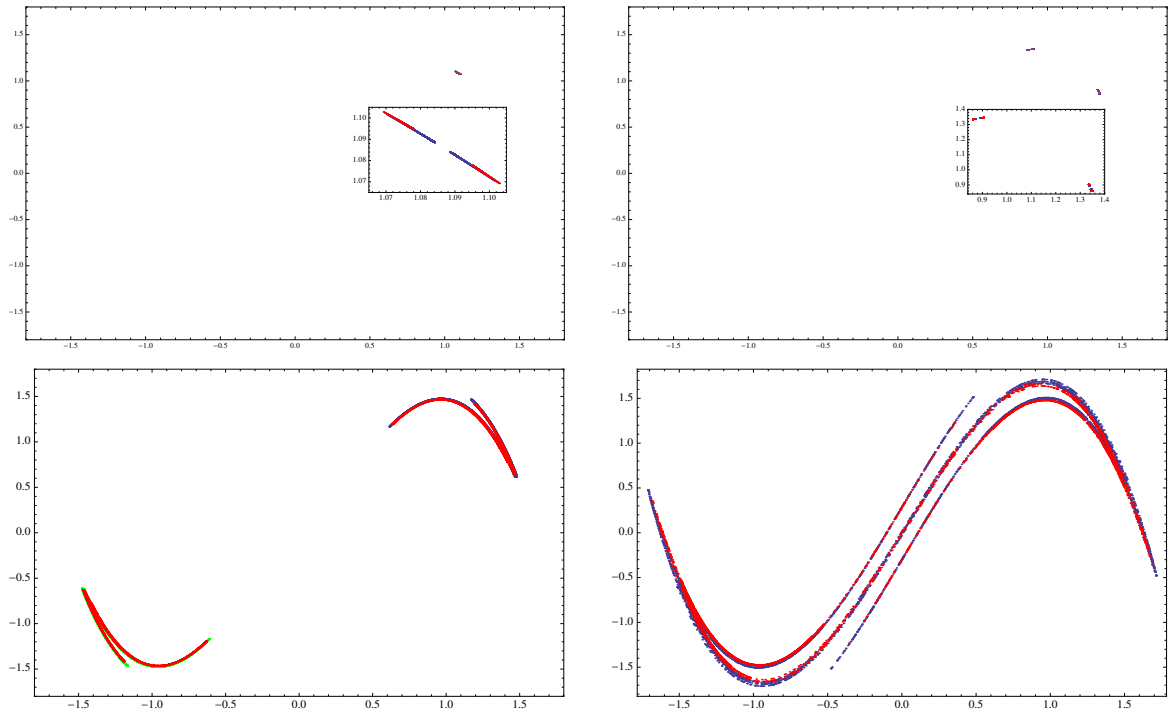

Fig. 4. Attractor reconstruction of the Duffing map from the original time series data in Fig. 2, displayed in blue. The reconstructed data are displayed in red for easier visual comparison: (t-l) two segment attractor; (t-r): four segment attractor; (b-l) two independent chaotic attractors; (b-r) a single chaotic attractor.

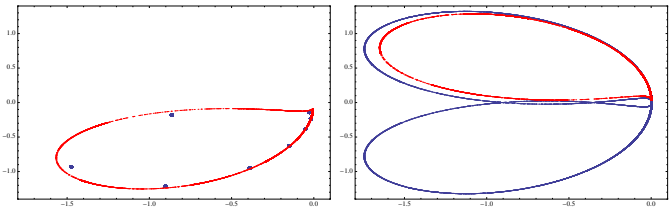

Fig. 5. Examples of inaccurate attractor reconstructions for the Burger map.

We should also acknowledge some limitations of our method. Although it demonstrates commendable accuracy in attractor reconstruction, there exists some discrepancy between the original and reconstructed data. For instance, in Fig. 3(top-right), the eight periodic points in blue and red are close but not identical. This disparity can be partly attributed to the extreme sensitivity of chaotic systems to initial conditions, as well as the stochastic nature of our method. To address this, all simulations must be repeated multiple times to mitigate the randomness inherent in certain parameters of the bat algorithm. In this study, we conducted 10 independent simulations for all input time series, selecting the best outcome for presentation. Nonetheless, individual executions may fail to accurately reconstruct the original attractor, as illustrated in Fig. 5 for the Burger map. On the left, the method returned a chaotic attractor in red for the original period-8 orbit in blue, while on the right, the original single attractor in blue has been reconstructed by the half-side chaotic attractor in red. These instances underscore the importance of performing multiple independent executions to ensure reliable performance.

V. Conclusions and Future Work

In this paper, a new method for reconstruction of periodic and chaotic attractors of low-dimensional dynamical systems from time series data is introduced. The method is based on a powerful bio-inspired swarm intelligence method called bat algorithm. The method has been applied to two illustrative examples of chaotic maps: the Burger map and the Duffing map. The graphical and numerical results show that the method performs well and is able to recover the underlying shape of the attractors of chaotic maps for a variety of periodic and chaotic behaviors with good accuracy. Some limitations of the method have also been exposed. Altogether, we can conclude that the presented approach is very promising for this relevant but challenging problem.

Despite these promising findings, our approach has certain limitations that require consideration. Firstly, the method is confined to low-dimensional maps, thereby limiting its applicability for high-dimensional systems. Additionally, the fitting of chaotic maps through an algebraic scheme may not be optimal for transcendental functions. Addressing these limitations requires further methodological research. Extending our method to more challenging scenarios, such as chaotic flows governed by sets of ordinary differential equations, represents an important direction for future work. Furthermore, applying our approach to the control and suppression of chaos [18], [24], [32] and the synchronization of chaotic systems [16], [33], would advance our understanding of chaotic phenomena. Future work will also involve conducting a comparative

analysis of our results against other metaheuristic techniques. Additionally, enhancing the bat algorithm through hybridization with a local search strategy, as in previous studies [11], is also part of our future work in the field.

ACKNOWLEDGMENT

The authors thank the project PDE-GIR of the European Union's Horizon 2020 research and innovation programme, Marie Sklodowska-Curie Actions program, grant 778035, and the grant PID2021-127073OB-I00 of the Agencia Estatal de Investigación (AEI) of the Spanish Ministry of Science and Innovation, MCIN/AEI/10.13039/501100011033/FEDER, EU.

REFERENCES

[1] H.D. Abarbanel, R. Brown, J.J. Sidorowich, L.S. Tsimring, The analysis of observed chaotic data in physical systems. *Reviews of Modern Physics*, vol. 65, pp. 1331–1392, 1993.

[2] G.L. Baker, J.P. Gollub, *Chaotic Dynamics: An Introduction*. Cambridge University Press, Cambridge, UK, 1990.

[3] C.S. Bertuglia, F. Vaio, *Nonlinearity, Chaos, and Complexity: The Dynamics of Natural and Social Systems*. Oxford University Press, Oxford, UK, 2005.

[4] J.M. Burgers: Mathematical examples illustrating relations occurring in the theory of turbulent fluid motion. *Trans. Roy. Neth. Acad. Sci. Amsterdam*, vol. 17, pp. 1–53, 1939.

[5] A. Campuzano, A. Iglesias, A. Gálvez, Free-form parametric fitting of van der Waals binodal and spinodal curves with bat algorithm. Proc. of 13th Int. Conf. on Software, Knowledge, Information Management and Applications (SKIMA), *IEEE Computer Society Press*, pp. 1–8, 2019.

[6] M. Casdagli, S. Eubank, J.D. Farmer, J. Gibson, State space reconstruction in the presence of noise. *Physica D: Nonlinear Phenomena*, vol. 51, pp. 52–98, 1991.

[7] R.L. Devaney, *An Introduction to Chaotic Dynamical Systems, Third Edition*. CRC Press, Boca Raton, FL, 2022.

[8] E. R. Deyle, G. Sugihara, Generalized theorems for nonlinear state space reconstruction. *PLoS One*, vol. 6, e18295, 2011.

[9] A. Gálvez, Numerical-symbolic Matlab program for the analysis of three-dimensional chaotic systems. *Lecture Notes in Computer Science*, vol. 4488, pp. 211–218, 2007.

[10] A. Gálvez, I. Fister Jr., E. Osaba, I. Fister, J.D. Ser, A. Iglesias, Computing rational border curves of melanoma and other skin lesions from medical images with bat algorithm. *Proc. Genetic and Evolutionary Computation Conf., ACM GECCO 2019*, ACM, pp. 1675-1682, 2019.

[11] A. Gálvez, A. Iglesias, J.A. Díaz, I. Fister, J. López, I. Fister Jr., Modified OFS-RDS bat algorithm for IFS encoding of bitmap fractal binary images. *Advanced Engineering Informatics*, vol. 47, Paper 101222, 2021.

[12] A. Gálvez, A. Iglesias, E. Osaba, J. del Ser, Bat algorithm method for automatic determination of color and contrast of modified digital images. *Prof. of 44th Annual Computers, Software, and Applications Conference, IEEE COMPSAC 2020*, pp. 1195–1200, 2020.

[13] Z. Ghahramani, S. T. Roweis, Learning nonlinear dynamical systems using an em algorithm. In *Advances in neural information processing systems*, 431–437, 1999.

[14] J. Güémez, J.M. Gutiérrez, A Iglesias, M.A. Matías, Stabilization of periodic and quasiperiodic motion in chaotic systems through changes in the system variables. *Physics Letters A*, 190 (5-6), 429–433, 1994.

[15] J. Güémez, J.M. Gutiérrez, A Iglesias, M.A. Matías, Suppression of chaos through changes in the system variables: transient chaos and crises. *Physica D: Nonlinear Phenomena*, 79 (2-4), 164–173, 1994.

[16] J.M. Gutiérrez, A. Iglesias, Synchronizing chaotic systems with positive conditional Lyapunov exponents by using convex combinations of the drive and response systems, *Physics Letters A*, vol. 239, Issue 3, pp. 174–180, 1998.

[17] J.M. Gutiérrez, A. Iglesias, A Mathematica package for the analysis and control of chaos in nonlinear systems, *Computers in Science and Engineering*, 12 (6), 608–619, 1998.

[18] J.M. Gutiérrez, A Iglesias, J Güémez, M.A. Matías, Suppression of chaos through changes in the system variables through Poincaré and Lorenz return maps, *International Journal of Bifurcation and Chaos*, vol. 6, Issue 7, pp. 1351–1362, 1996.

[19] R. Hilborn, *Chaos and Nonlinear Dynamics: An Introduction for Scientists and Engineers*. Oxford University Press, Oxford, UK, 2001.

[20] G. E. Hinton, R. R. Salakhutdinov, Reducing the dimensionality of data with neural networks. *Science*, 313, 504–507, 2006.

[21] P. Holmes: A nonlinear oscillator with a strange attractor. *Philosophical Transactions of the Royal Society A*, vol. 292, issue 1394, pp. 419–448, 1979.

[22] A. Iglesias, A. Gálvez, M. Collantes, Multilayer embedded bat algorithm for B-spline curve reconstruction. *Integrated Computer-Aided Engineering*, vol. 24(4), pp. 385–399, 2017.

[23] A. Iglesias, A. Gálvez, M. Collantes, Iterative sequential bat algorithm for free-form rational Bézier surface reconstruction. *International Journal of Bio-Inspired Computation*, vol. 11(1), pp. 1–15, 2018.

[24] A. Iglesias, J.M. Gutiérrez, J. Güémez, M.A. Matías, Chaos suppression through changes in the system variables and numerical rounding errors, *Chaos, Solitons and Fractals*, vol. 7, Issue 8, pp. 1305–1316, 1996.

[25] H. Jiang, H. He, State space reconstruction from noisy nonlinear time series: An autoencoder-based approach. In: *Proc. International Joint Conference on Neural Networks (IJCNN)*, IEEE, 3191–3198, 2017.

[26] M. Karl, M. Soelch, J. Bayer, P. Van der Smagt, Deep variational Bayes filters: Unsupervised learning of state space models from raw data. In: *Proc. Int. Conf. on Learning Representations*, 1–13, 2017.

[27] M. B. Kennel, R. Brown, H.D. Abarbanel, Determining embedding dimension for phase-space reconstruction using a geometrical construction. *Physical Review A*, vol. 45, pp. 3403–3411, 1992.

[28] Z. Lu, B.R. Hunt, E. Ott, Attractor reconstruction by machine learning. *Chaos: An Interdisciplinary Journal of Nonlinear Science*, 28, Paper 061104, 2018.

[29] B. Lusch, J.N. Kutz, S.L. Brunton, Deep learning for universal linear embeddings of nonlinear dynamics. *Nature Commun.*, 9, 1–10, 2018.

[30] P. Mellodge, *A Practical Approach to Dynamical Systems for Engineers, 1st ed.*, Elsevier, Amsterdam, The Netherlands, 2015.

[31] K.R. Müller, A.J. Smola, G. Rätsch, B. Schölkopf, J. Kohlmorgen, V. Vapnik, Predicting time series with support vector machines. In: *Proc. of International Conference on Artificial Neural Networks*, 999–1004, Springer, 1997.

[32] E. Ott, C. Grebogi, J. Yorke, J., Controlling chaos. *Physical Review Letters*, vol. 64 (11), pp. 1196–1199, 1990.

[33] L.M. Pecora, T.L. Carroll, Synchronization in chaotic systems. *Physical Review Letters*, vol. 64, pp. 821–823, 1990.

[34] S.S. Rangapuram, M. Seeger, J. Gasthaus, L. Stella, Y. Wang, T. Januschowski. Deep state space models for time series forecasting. In: *Proc. of the 32nd Int. Conf. on Neural Information Processing Systems*, ACM Press, 7785–7794, 2018.

[35] Q. She, Y. Gao, K. Xu, R.H. Chan, Reduced-rank linear dynamical systems. In:*Proc. of Thirty-Second AAAI Conference on Artificial Intelligence*, ACM Press, 4050–4057, 2018.

[36] S.H. Strogatz, *Nonlinear Dynamics and Chaos: With Applications to Physics, Biology, Chemistry, and Engineering, 2nd ed.*, CRC Press, Boca Raton, FL, 2015.

[37] P. Suárez, A. Iglesias, Bat algorithm for coordinated exploration in swarm robotics. *Prof. of 8th Int. Conf. ICSI 2017*, pp. 176–184, 2017.

[38] P. Suárez, A. Iglesias, A. Gálvez, Autonomous coordinated navigation of virtual swarm bots in dynamic indoor environments by bat algorithm. *Prof. of 3rd Int. Conf. ICHSA 2017*, pp. 134–144, 2017.

[39] P. Suárez, A. Iglesias, A. Gálvez, Make robots be bats: specializing robotic swarms to the bat algorithm. *Swarm and Evolutionary Computation*, vol. 44, pp. 113–129, 2019.

[40] J.M.T. Thompson, H.B. Stewart, *Nonlinear Dynamics and Chaos, 2nd ed.*, John Wiley & Sons, Hoboken, NJ, 2002.

[41] R. R. Whitehead, N. MacDonald, A chaotic map that displays its own homoclinic structure. *Physica D*, vol. 13, pp. 401–408, 1984.

[42] R. R. Whitehead, N. MacDonald, Introducing students to nonlinearity: computer experiments with Burgers mappings. *European Journal of Physics*, vol. 6, pp. 143–147, 1985.

[43] X.S. Yang, A new metaheuristic bat-inspired algorithm. *Studies in Computational Intelligence*, Springer Berlin, vol. 284, pp. 65–74, 2010.

[44] X.S. Yang, Bat algorithm: literature review and applications. *Int. Journal of Bio-Inspired Computation*, vol. 5(3), pp. 141–149, 2013.

[45] X.S. Yang, A.H. Gandomi, Bat algorithm: a novel approach for global engineering optimization. *Engineering Computations*, vol. 29(5), pp. 464–483, 2012.